

# Non-ideal self-gravity and cosmology: the importance of correlations in the dynamics of the large-scale structures of the Universe

P. Tremblin<sup>1\*</sup>, G. Chabrier<sup>2,3</sup>, T. Padioleau<sup>1</sup>, and S. Daley-Yates<sup>1</sup>

<sup>1</sup> Maison de la Simulation, CEA, CNRS, Univ. Paris-Sud, UVSQ, Université Paris-Saclay, F-91191 Gif-sur-Yvette, France

<sup>2</sup> Ecole Normale Supérieure de Lyon, CRAL, UMR CNRS 5574, 69364 Lyon Cedex 07, France

<sup>3</sup> Astrophysics Group, University of Exeter, EX4 4QL Exeter, UK

Received ### # 2019; accepted ### #, 2019

## ABSTRACT

**Aims.** Inspired by the statistical mechanics of an ensemble of interacting particles (BBGKY hierarchy), we propose to account for small-scale inhomogeneities in self-gravitating astrophysical fluids by deriving a non-ideal Virial theorem and non-ideal Navier-Stokes equations. These equations involve the pair radial distribution function (similar to the two-point correlation function used to characterize the large-scale structures of the Universe), similarly to the interaction energy and equation of state in liquids. Within this framework, small-scale correlations lead to a non-ideal amplification of the gravitational interaction energy, whose omission leads to a missing mass problem, e.g., in galaxies and galaxy clusters.

**Methods.** We propose to use a decomposition of the gravitational potential into a near- and far-field component in order to account for the gravitational force and correlations in the thermodynamics properties of the fluid. Based on the non-ideal Virial theorem, we also propose an extension of the Friedmann equations in the non-ideal regime and use numerical simulations to constrain the contribution of these correlations to the expansion and acceleration of the Universe.

**Results.** We estimate the non-ideal amplification factor of the gravitational interaction energy of the baryons to lie between 5 and 20, potentially explaining the observed value of the Hubble parameter (since the uncorrelated energy account for  $\sim 5\%$ ). Within this framework, the acceleration of the expansion emerges naturally because of the increasing number of sub-structures induced by gravitational collapse, which increases their contribution to the total gravitational energy. A simple estimate predicts a non-ideal deceleration parameter  $q_{\text{ni}} \simeq -1$ ; this is potentially the first determination of the observed value based on an intuitively physical argument. We also suggest that small-scale gravitational interactions in bound structures (spiral arms or local clustering) could yield a transition to a viscous regime that can lead to flat rotation curves. This transition could also explain the dichotomy between (Keplerian) LSB elliptical galaxy and (non-Keplerian) spiral galaxy rotation profiles. Overall, our results demonstrate that non-ideal effects induced by inhomogeneities must be taken into account, potentially with our formalism, in order to properly determine the gravitational dynamics of galaxies and the larger scale universe.

**Key words.** gravitation, equation of state, cosmology: theory

## 1. Introduction

Astrophysical flows are by nature multi-scale systems exhibiting a large range of dynamical regimes whose understanding remains quite challenging. Since the 70s/80s, hydro or N-body high performance numerical simulations have been key tools to understand self-gravitating systems. However, a proper understanding of collective effects in such simulations remain challenging because, notably, of numerical artifacts. Therefore, theory remains vital for assessing the genuine validity of the numerical simulations.

The theoretical description of an ensemble of particles is a challenging task that has motivated the development of a major domain in physics: statistical mechanics. The statistical descriptions of a gas and a solid are relatively easy in two limit cases: perfect disorder, often referred to as molecular chaos for ideal gases, or perfect order for ordered solids. The description of liquids, or ill-condensed systems, however, is much more complex and has only been possible after the pioneering work of Bo-

golyubov, Born, Green, Kirkwood, and Yvon, referred to as the BBGKY hierarchy (e.g. Yvon 1935; Born & Green 1946; Bogoliubov 1946; Kirkwood 1946). Within this framework, the ensemble of particles is described by the one-particle probability density function, the two-particle probability density function, and so on. Truncated at the second order, the system is described by the one-particle density function and the pair correlation function, generally referred to as the radial distribution function in liquid statistical mechanics. In the case of perfect chaos for an ideal gas, the radial distribution function is uniformly equal to 1, which means that there is no correlation in the fluid: the probability of finding two particles at two given points is equal to the product of the probabilities of finding one particle at these given points.

Liquids differ from an ideal gas because of the presence of inter-particle forces that lead to correlations at short distances and they differ from solids because of the lack of (periodic) long-range order (i.e. the pair correlation function tends to 1 at long distance). For water, the dominant effects responsible for these inter-molecular forces are dipolar interactions and hydrogen bonding. Many other processes can be at play and make

\* e-mail: pascal.tremblin@cea.fr

the picture more complex. However, from a statistical point of view the knowledge of the radial distribution function is sufficient to derive the thermodynamic properties of the fluid, such as the equation of state (see Hansen & McDonald 2006; Aslanoglu 2006).

Most of the developments of liquid statistical mechanics deeply rely on the fact that the interactions at play are short-range: even though the interaction energy is proportional to the number of particle pairs in the fluid, only the close neighbors actually matter. This allows to find an extensive definition of the interaction energy that does not diverge in the thermodynamic limit. A noticeable exception is the case of Coulombic fluids, which interact throughout the Coulomb potential ( $\propto 1/r$ ); large-scale convergence in that case is insured by the neutralizing electron background. Unfortunately, this (screening) property is not met by a self-gravitating fluid since the gravitational force is a priori non-extensive and always attractive: the interaction energy is a priori non-extensive and requires possibly a new extension of statistical mechanics to include non-extensive hierarchical systems (see, e.g. de Vega & Sánchez 2002; Pfenniger 2006). This prevents astrophysicists from benefiting from the insight found from developments of statistical mechanics in the presence of interactions. For this reason, at large scales such as galaxies or the large-scale structures of the Universe, the gravitational interactions of unresolved structures in the simulations are usually ignored or neglected, resulting from the use of an ideal gas approximation when calculating the thermodynamic properties of the fluid. Such an approximation, however, can lead to inconsistencies in our description of the Universe.

The present paper aims at proposing to properly apply statistical mechanics to gravitational systems by solving the problem of non-extensivity. This leads to the derivation of a non-ideal Virial theorem and non-ideal Navier-Stokes equations to be used for self-gravitating hydrodynamic fluids when, as is the case within the universe, correlations due to self-gravitating substructures are present. In Sect. 2, we recall classical results of statistical mechanics in order to define a non-ideal equation of state (EOS) in the presence of interactions. In Sect. 3, we propose a way to adapt these tools to the long-range gravitational force by using a near-field and far-field decomposition of the potential. In Sect. 4, we present a semi-analytical example using polytropic stellar structures to illustrate the importance of inhomogeneities and correlations when computing the correct interaction energy in the Virial theorem. Then, we explore the role of the gravitational force and the correlations at small scales in galaxies to explain the observed flat rotation curves. Finally, using for now the Newtonian limit, we define non-ideal Friedmann equations and explore the possible consequences of these non-ideal effects in the context of the expanding and accelerating Universe. In Sect. 5 we summarize our conclusions, we discuss the limitations of our work and we propose ways to go further in exploring this potentially interesting idea.

## 2. Statistical mechanics of an ensemble of interacting particles

### 2.1. BBGKY hierarchy

Following the work of Bogolyubov, Born, Green, Kirkwood, and Yvon, known as the BBGKY hierarchy, we introduce some notations of statistical mechanics. We consider  $N$  particles of mass  $m$  within a volume  $V$ . We can define  $P_s(\mathbf{r}_1, \mathbf{r}_2, \dots, \mathbf{r}_s)$  the probability to find  $s$  particles at the positions  $(\mathbf{r}_1, \mathbf{r}_2, \dots, \mathbf{r}_s)$ . These probability density functions are normalized by the total number of  $N$ -uplets

$N^s$ . Two probability functions play an important role when there is no interaction involving more than two particles:  $P_1(\mathbf{r})$ , the probability to find one particle at  $\mathbf{r}$  and  $P_2(\mathbf{r}, \mathbf{r}')$ , the probability to find one particle at  $\mathbf{r}$  and one particle at  $\mathbf{r}'$ . These two probability functions can be used to define exactly fluid quantities involving one and two particles from their  $N$ -body counterparts.

For instance, using  $P_1(\mathbf{r})$ , we can define equivalently the total acceleration  $\langle \mathbf{a} \rangle$  of the fluid volume  $V$  and the sum of all the  $N$ -body particle accelerations:

$$\begin{aligned} \langle \mathbf{a} \rangle &= \sum_i \mathbf{a}_i \\ &= N \int_V \mathbf{a}(\mathbf{r}) P_1(\mathbf{r}) dV \end{aligned} \quad (1)$$

The use of  $P_1(\mathbf{r})$ , here, involves to counting the number of particles in the volume  $V$  since by definition the density inside the fluid volume is:

$$\rho(\mathbf{r}) = N P_1(\mathbf{r}). \quad (2)$$

In the case of a homogeneous and isotropic fluid,  $P_1(\mathbf{r})$  is simply equal to  $1/V$  for all  $\mathbf{r}$  and  $\rho$  is equal to  $N/V$ , the number density.

Similarly, one can define the interaction energy of the ensemble of particles  $\langle H_{\text{int}} \rangle$ : by summing all the interaction energies between distinct pairs of particles in the  $N$ -body description or by integrating over  $P_2(\mathbf{r}, \mathbf{r}')$  for the fluid volume.

$$\begin{aligned} \langle H_{\text{int}} \rangle &= \sum_{i < j} \phi(|\mathbf{r}_i - \mathbf{r}_j|) \\ &= \frac{N(N-1)}{2} \iint_{V,V} \phi(|\mathbf{r} - \mathbf{r}'|) P_2(\mathbf{r}, \mathbf{r}') dV dV', \end{aligned} \quad (3)$$

where  $N(N-1)/2$  is the number of independent pairs in the fluid. In the homogeneous and isotropic case,  $P_2(\mathbf{r}, \mathbf{r}')$  only depends on the distance modulus  $\|\mathbf{r} - \mathbf{r}'\|$ . It is then convenient to define the radial distribution function

$$g(\|\mathbf{r} - \mathbf{r}'\|) = V^2 P_2(\mathbf{r}, \mathbf{r}'), \quad (4)$$

or equivalently the correlation function,  $\xi(\|\mathbf{r} - \mathbf{r}'\|)$ , for a homogeneous isotropic fluid:

$$\begin{aligned} \xi(\|\mathbf{r} - \mathbf{r}'\|) &= V^2 (P_2(\mathbf{r}, \mathbf{r}') - P_1(\mathbf{r}) P_1(\mathbf{r}')) \\ &= V^2 P_2(\mathbf{r}, \mathbf{r}') - 1 \\ &= g(\|\mathbf{r} - \mathbf{r}'\|) - 1. \end{aligned} \quad (5)$$

For an isotropic fluid, the correlation function  $\xi(r)$  is the angle-averaged value of  $\xi(\mathbf{r}) = \langle \delta(\mathbf{r}') \delta(\mathbf{r} + \mathbf{r}') \rangle$ , with  $\delta(\mathbf{r})$  the density perturbation defined as  $\delta(\mathbf{r}) = (\rho(\mathbf{r}) - \langle \rho \rangle) / \langle \rho \rangle$  (see Springel et al. 2017). Here,  $\langle \cdot \rangle$  denotes a volume average. The power spectrum can then be defined as the Fourier transform of  $\xi(\mathbf{r})$ :

$$\xi(\mathbf{r}) = \frac{V}{(2\pi)^3} \int |\delta_{\mathbf{k}}|^2 e^{-i\mathbf{k} \cdot \mathbf{r}} d^3k, \quad (6)$$

which is commonly used in cosmological studies to characterize the large-scale structures of the Universe (Peebles 1980; Peacock 1999). In this paper, we will show that the correlation function is not a simple diagnostic of structures but that it plays an active role determining the dynamics of the fluid. For the sake of similarity with the usual tools used in statistical physics, we will use

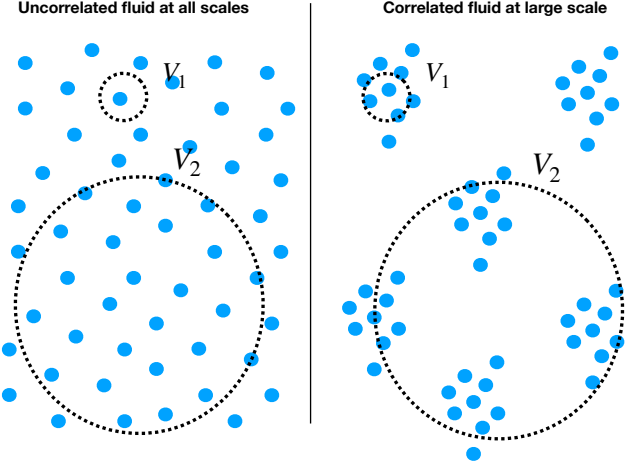


Fig. 1: Schematic illustration of situations when the ideal hypothesis is valid and when it breaks down. Left: the fluid is uncorrelated at all scales. Right: on the scale of the control volume  $V_1$ , the fluid can be considered locally as inhomogeneous and uncorrelated while on the scale of the control volume  $V_2$ , the fluid can be considered as globally homogeneous and correlated.

the radial distribution function rather than the correlation function in our calculations.

It is easy to see that in the absence of correlation in the fluid:  $P_2(\mathbf{r}, \mathbf{r}') = P_1(\mathbf{r})P_1(\mathbf{r}')$ , i.e.  $\xi(\|\mathbf{r} - \mathbf{r}'\|) = 0$  and  $g(\|\mathbf{r} - \mathbf{r}'\|) = 1$  for all  $\mathbf{r}$  and  $\mathbf{r}'$  in the case of a homogeneous fluid. This situation is the limit case of an ideal fluid, often referred to as “perfect molecular chaos”, for which the radial distribution function is equal to 1 everywhere. A schematic representation of such an ideal and homogeneous fluid is portrayed in the left panel of Fig. 1, where the blue dots represent point-like interactionless particles. In this example the fluid is homogeneous at all scales: the density inside a small ( $V_1$ ) or large ( $V_2$ ) control volume is independent of the location of the control volume.

In the presence of interactions, the density distribution may no longer be homogeneous at all scales, e.g. in the presence of clustering in the particle distribution. Such a situation is shown in the right panel of Fig. 1:

- for a small control volume  $V_1$ , the distribution of particles within the volume is ideal and there is no correlation:  $P_2(\mathbf{r}, \mathbf{r}') = P_1(\mathbf{r})P_1(\mathbf{r}')$ . However, the density will depend on the location of the control volume, e.g. if it lies within a cluster or outside. This means that inhomogeneities are resolved and the fluid is ideal (i.e. uncorrelated) but inhomogeneous.
- for a large control volume  $V_2$ , the distribution of particles within the volume is not ideal and there are correlations induced by the clustering inside the volume:  $P_2(\mathbf{r}, \mathbf{r}') \neq P_1(\mathbf{r})P_1(\mathbf{r}')$ . However the density will not depend on the location of the control volume provided that the control volume is sufficiently large. In that case, the inhomogeneities are not resolved and the fluid is non-ideal (correlated) and homogeneous.

This distinction is very important for the correct treatment of inhomogeneities (correlations) in a fluid. Since it depends on the scale, this is of prime importance for astrophysical flows, that can only be observed or simulated at large scales. The main consequence is that one cannot simply average over large

volumes as this masks the complexity of the density inhomogeneities: these inhomogeneities then result in correlations in the fluid that requires a change to the dynamical equations. This can be seen with the computation of the interaction energy, which depends intrinsically on the distance between particles (see Eq. 3). Within a statistical (fluid) description, the interaction energy fundamentally involves the pair correlation function,  $P_2(\mathbf{r}, \mathbf{r}') \neq P_1(\mathbf{r})P_1(\mathbf{r}')$ . In a simulation assuming an ideal fluid, the correlations will be missed, i.e. the fluid at small scale may erroneously be considered as ideal if correlations are present, yielding an erroneous estimate of the interaction energy. The proper calculation of this latter must thus be done accurately, making sure the small-scale interaction energy is properly accounted for, potentially through Eq. 3 and the use of a non-ideal framework.

## 2.2. Virial theorem for correlated fluids

For a system of interacting particles of mass  $m$ , the N-body form of the Virial theorem can be stated as:

$$-\sum_i m v_i^2 + \frac{1}{2} \sum_i \frac{d^2 I_i}{dt^2} = \sum_{i,j,i \neq j} \mathbf{F}_{j \rightarrow i} \cdot \mathbf{r}_i \quad (7)$$

where  $I_i = m r_i^2$  is the moment of inertia of the particle  $i$ . In a fluid (statistical) approach, the equivalent form reads:

$$\begin{aligned} -N \int_V m v^2(\mathbf{r}) P_1(\mathbf{r}) dV + \frac{1}{2} N \int_V \frac{d^2 I}{dt^2}(\mathbf{r}) P_1(\mathbf{r}) dV \\ = N(N-1) \iint_{V,V'} \mathbf{F}_{\mathbf{r}' \rightarrow \mathbf{r}} \cdot \mathbf{r} P_2(\mathbf{r}, \mathbf{r}') dV dV'. \end{aligned} \quad (8)$$

Assuming a force deriving from a potential  $\phi \propto |\mathbf{r} - \mathbf{r}'|^\alpha$ , the last integral can be symmetrized by using  $P_2(\mathbf{r}, \mathbf{r}') = P_2(\mathbf{r}', \mathbf{r})$  to get

$$\begin{aligned} N(N-1) \iint_{V,V'} \mathbf{F}_{\mathbf{r}' \rightarrow \mathbf{r}} \cdot \mathbf{r} P_2(\mathbf{r}, \mathbf{r}') dV dV' \\ = \frac{N(N-1)}{2} \iint_{V,V'} \mathbf{F}_{\mathbf{r}' \rightarrow \mathbf{r}} \cdot (\mathbf{r} - \mathbf{r}') P_2(\mathbf{r}, \mathbf{r}') dV dV' \\ = -\alpha \frac{N(N-1)}{2} \iint_{V,V'} \phi(|\mathbf{r} - \mathbf{r}'|) P_2(\mathbf{r}, \mathbf{r}') dV dV' \end{aligned} \quad (9)$$

in which we recognize the interaction energy defined in Eq. 3. The Virial theorem takes now the classic form

$$\langle m v^2 \rangle - \alpha \langle H_{\text{int}} \rangle = \frac{\langle d^2 I / dt^2 \rangle}{2} \quad (10)$$

in which we note the presence of the pair correlation function in the interaction energy.

Similarly, we can define the total mechanical energy  $E_m$  of the N-body ensemble of particles

$$\begin{aligned} E_m &= \langle m v^2 / 2 \rangle + \langle H_{\text{int}} \rangle \\ &= \frac{1}{2} \sum_i m v_i^2 + \sum_{i < j} \phi(|\mathbf{r}_i - \mathbf{r}_j|), \end{aligned} \quad (11)$$

whose fluid counterpart is given by

$$E_m = \frac{N}{2} \int_V m v^2(\mathbf{r}) P_1(\mathbf{r}) dV + \frac{N(N-1)}{2} \iint_{V,V'} \phi(|\mathbf{r} - \mathbf{r}'|) P_2(\mathbf{r}, \mathbf{r}') dV dV'. \quad (12)$$

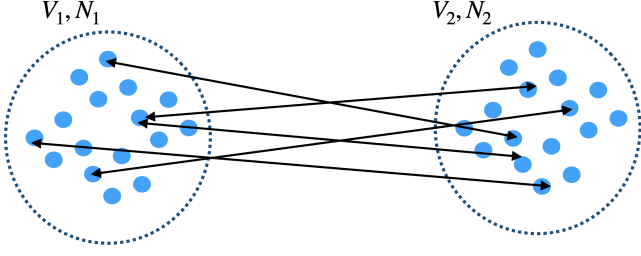


Fig. 2: Schematic illustrating the interactions between two fluid volumes used for the derivation of Newton’s laws for pressureless correlated fluids.

If we neglect correlations in the interaction energy, then  $P_2(\mathbf{r}, \mathbf{r}') = P_1(\mathbf{r})P_1(\mathbf{r}')$ , which yields, in the limit  $N \gg 1$

$$\begin{aligned} \langle H_{\text{int}} \rangle &\approx \frac{N^2}{2} \iint_{V,V'} \phi(|\mathbf{r} - \mathbf{r}'|) P_1(\mathbf{r}) P_1(\mathbf{r}') dV dV' \\ &\approx \frac{1}{2} \iint_{V,V'} \phi(|\mathbf{r} - \mathbf{r}'|) \rho(\mathbf{r}) \rho(\mathbf{r}') dV dV' \\ &\approx \frac{1}{2} \int_V \rho(\mathbf{r}) \Phi(\mathbf{r}) dV, \end{aligned} \quad (13)$$

where we have defined the mean-field potential  $\Phi(\mathbf{r}) = \int_V \phi(|\mathbf{r} - \mathbf{r}'|) \rho(\mathbf{r}') dV'$ , which can be computed with the Poisson equation for the gravitational or the electrostatic force,  $\nabla^2 \Phi(\mathbf{r}) \propto \rho(\mathbf{r})$ . However, we stress that the possibility to define this mean-field potential is only possible in the absence of correlations: as soon as  $P_2(\mathbf{r}, \mathbf{r}') \neq P_1(\mathbf{r})P_1(\mathbf{r}')$ , the use of a mean-field and the Poisson equation is not correct as it will ignore the correlations present in the system.

### 2.3. Newton’s laws of motion for pressureless correlated fluids

At a more fundamental level, we can also show that correlations should be taken into account in Newton’s laws for a (pressureless) correlated fluid. We consider now an ensemble of  $N_1$  particles of mass  $m_1$  in a volume  $V_1$  interacting with  $N_2$  particles of mass  $m_2$  in a volume  $V_2$  (see Fig. 2). In an N-body approach, the second law can be written

$$\sum_i m_1 \mathbf{a}_i = \sum_{j,i} \mathbf{F}_{j \rightarrow i}, \quad (14)$$

with  $i$  in  $[0, N_1]$  and  $j$  in  $[0, N_2]$ . The Newton’s second law for a pressureless correlated fluid is then given by

$$N_1 \int_{V_1} m_1 \mathbf{a}(\mathbf{r}) P_1(\mathbf{r}) dV_1 = N_1 N_2 \iint_{V_1, V_2} \mathbf{F}_{\mathbf{r}_2 \rightarrow \mathbf{r}_1} P_2(\mathbf{r}_1, \mathbf{r}_2) dV_1 dV_2, \quad (15)$$

which we write in a more compact way as  $\langle m_1 \mathbf{a} \rangle_1 = \langle \mathbf{F} \rangle_{2 \rightarrow 1}$ . Note that we have generalized the two-point probability density function to different volumes  $V_1$  and  $V_2$  and it is normalized by  $N_1 N_2$ .

The first law for an isolated fluid of volume  $V_1$  is then  $\langle m_1 \mathbf{a} \rangle_1 = \langle \mathbf{F} \rangle_{1 \rightarrow 1} = 0$  and can be deduced from the second law by taking  $V_2 = V_1$  and using  $P_2(\mathbf{r}_1, \mathbf{r}'_1) = P_2(\mathbf{r}'_1, \mathbf{r}_1)$  and  $\mathbf{F}_{\mathbf{r}_1 \rightarrow \mathbf{r}'_1} = -\mathbf{F}_{\mathbf{r}'_1 \rightarrow \mathbf{r}_1}$ . Similarly, one can get the third law  $\langle \mathbf{F} \rangle_{2 \rightarrow 1} = -\langle \mathbf{F} \rangle_{1 \rightarrow 2}$  using the same arguments.

Let us assume now that there is no correlation, i.e.  $P_2(\mathbf{r}_1, \mathbf{r}_2) = P_1(\mathbf{r}_1)P_1(\mathbf{r}_2)$ , and that the fluid is isotropic and homogeneous.:  $P_1(\mathbf{r}_1) = 1/V_1$ . Choosing the origin of positions,  $\mathbf{x}$ , at the center of  $V_1$ , we have  $N_1/V_1 = \rho_1(\mathbf{x})$  (see Sect. 2.1) and we define

$$\begin{aligned} \mathbf{a}(\mathbf{x}) &= \frac{1}{V_1} \int_{V_1} \mathbf{a}(\mathbf{r}) dV_1, \\ \Phi(\mathbf{x}) &= \frac{1}{V_1} \iint_{V_1, V_2} \phi(|\mathbf{r}_2 - \mathbf{r}_1|) \rho_2(\mathbf{r}_2) dV_1 dV_2. \end{aligned} \quad (16)$$

The second law then becomes

$$\begin{aligned} \frac{\rho_1(\mathbf{x}) m_1}{V_1} \int_{V_1} \mathbf{a}(\mathbf{r}) dV_1 &= \frac{\rho_1(\mathbf{x}) m_1}{V_1} \iint_{V_1, V_2} \frac{\mathbf{F}_{\mathbf{r}_2 \rightarrow \mathbf{r}_1}}{m} \rho_2(\mathbf{r}_2) dV_1 dV_2 \\ \rho_1(\mathbf{x}) m_1 \mathbf{a}(\mathbf{x}) &\approx \rho_1(\mathbf{x}) m_1 \frac{-\nabla_{\mathbf{x}} \Phi(\mathbf{x})}{m_1}, \end{aligned} \quad (17)$$

where one recognizes now the usual form of an external mean force deriving from the mean field potential  $\Phi(\mathbf{x})$ . In the case of the gravitational force,  $\Phi(\mathbf{x})/m_1$  is independent of  $m_1$  and we see that the equivalence principle for a pressureless ideal fluid consists simply in simplifying Eq. 17 by  $\rho_1(\mathbf{x}) m_1$  on each side:

$$\mathbf{a}(\mathbf{x}) \approx \frac{-\nabla_{\mathbf{x}} \Phi(\mathbf{x})}{m_1}. \quad (18)$$

However, this simplification is only possible in the absence of correlations i.e. as soon as  $P_2(\mathbf{r}, \mathbf{r}') \neq P_1(\mathbf{r})P_1(\mathbf{r}')$ , the use of the equivalence principle is not correct as it will ignore the correlations present in the system.

### 2.4. Non-ideal equation of state

We recall that for a homogeneous and isotropic fluid,  $P_2(\mathbf{r}, \mathbf{r}') = g(|\mathbf{r} - \mathbf{r}'|)/V^2$ . In that case (for  $N \gg 1$ ), the interaction energy becomes

$$\langle H_{\text{int}} \rangle = \frac{2\pi N^2}{V} \int_0^R g(r) \phi(r) r^2 dr, \quad (19)$$

with  $r = |\mathbf{r} - \mathbf{r}'|$  and  $V = 4\pi R^3/3$ . One can use statistical mechanics in the canonical ensemble in thermal equilibrium with a heat bath at a fixed temperature  $T$  to define the EOS. We refer the reader to classical textbooks such as Hansen & McDonald (2006) for details. The energy of the system in the absence of external forces is then given by:

$$E = \frac{Nk_B T}{\gamma - 1} + \frac{2\pi N^2}{V} \int_0^R g(r) \phi(r) r^2 dr, \quad (20)$$

with  $\gamma = C_P/C_V$  the adiabatic index of the fluid, defined as the ratio of the specific heats at constant pressure and volume, respectively ( $\gamma = 5/3$  for mono-atomic particles in their ground state). The first term in Eq. 20 is the perfect gas contribution whereas the second term stems from the interactions between particles. The non-ideal pressure is given by:

$$PV = Nk_B T - \frac{2\pi N^2}{3V} \int_0^R g(r) \frac{d\phi(r)}{dr} r^3 dr. \quad (21)$$

If one identifies the temperature with the velocity dispersion of particles within the fluid ( $k_B T = 1/2 \langle m v_i^2 \rangle$ ), Eq. 21 can be interpreted as the isotropic form of the Virial theorem.  $P = 0$  corresponds to Virial equilibrium, for which the ideal pressure is balanced by the interaction contribution.  $P > 0$  corresponds to a fluid that expands because either the ideal (kinetic) pressure dominates the interaction one or the interactions are repulsive,  $d\phi(r)/dr < 0$ . In contrast,  $P < 0$  corresponds to a fluid that collapses because the contribution due to attractive interactions  $d\phi(r)/dr > 0$  dominates the ideal one. This case corresponds for instance to a phase transition from gas to liquid, with the attractive interactions being the intermolecular dipole forces, or to gravitational collapse in the case of the gravitational force (see, e.g. de Vega & Sánchez 2002).

Strictly speaking, a self-interacting fluid should always be described with a non-ideal EOS. Nevertheless, an ideal approximation is possible if the interaction term is negligible in Eq. 21. Indeed, in that case  $g(r) \approx 1$ , so that, with  $\rho = N/V$ , the condition becomes

$$\rho k_B T \gg \frac{2\pi\rho^2}{3} \int_0^R \frac{d\phi(r)}{dr} r^3 dr. \quad (22)$$

For a potential of the form  $\phi = -k/r$  (with  $k > 0$  for the gravitational force or attractive Coulomb interactions)

$$\rho k_B T \gg \pi\rho^2 k R^2 / 3 \Rightarrow R \ll \sqrt{\frac{k_B T}{k\rho}}. \quad (23)$$

In this case, one can recognize the characteristic Debye screening length in the case of Coulomb interactions or the Jeans length in the case of the gravitational force. The condition in Eq. 23 states that an ideal approximation in the treatment of the fluid under consideration is acceptable if (and only if) the volumes considered are sufficiently small so that the Debye length or the Jeans length is well-resolved. Whereas such a condition is usually fulfilled in numerical simulations of star formation, and is known as the 'Truelove condition' (see Truelove et al. 1997), it is not easily done for large-scale numerical simulations of galaxies or larger structures. In these cases, it is mandatory to use a non-ideal EOS, thus to include in the calculations the terms involving the pair-correlation function.

### 2.5. Non-ideal stress tensor

More generally, one can express the above theory in the form of a stress tensor, following the pioneering work of Kirkwood et al. (1949). The Newtonian expression for the stress tensor of a system of  $N$  particles of mass  $m$ , is given by

$$\sigma_{ij} = - \left( P + \left( \frac{2}{3}\eta - \chi \right) \sum_k \partial_k u_k \right) \delta_{ij} + \eta (\partial_i u_j + \partial_j u_i), \quad (24)$$

with  $P$  the non-ideal pressure given in Sect. 2.4 and  $\eta$  and  $\chi$  the coefficients of shear and bulk viscosity that can be computed as

$$\begin{aligned} \eta &= \frac{1}{2} \frac{N}{V} m D + \frac{\pi}{15D} \frac{N^2}{V^2} \int_0^R \psi_2(r) g(r) \frac{d\phi(r)}{dr} r^3 dr, \\ \chi &= \frac{1}{3} \frac{N}{V} m D + \frac{\pi}{9D} \frac{N^2}{V^2} \int_0^R \psi_0(r) g(r) \frac{d\phi(r)}{dr} r^3 dr, \end{aligned} \quad (25)$$

with  $D$  the self-diffusion coefficient in the fluid (from Fick's law). As defined in Kirkwood et al. (1949),  $\psi_0(r)$  is the surface

harmonic of zeroth order arising from the dilatation component of the rate of strain, and  $\psi_2(r)$  is the surface harmonic of order 2 arising from the shear component. They obey the following differential equations

$$\begin{aligned} \frac{d}{dr} \left( r^2 g(r) \frac{d\psi_2(r)}{dr} \right) - 6\psi_2(r) g(r) &= r^3 \frac{dg(r)}{dr} \\ \frac{d}{dr} \left( r^2 g(r) \frac{d\psi_0(r)}{dr} \right) &= r^3 \frac{dg(r)}{dr}. \end{aligned} \quad (26)$$

As for the non-ideal pressure, the non-ideal coefficients of shear and bulk viscosity contain two contributions: an ideal (Brownian) one arising from the momentum transfer between colliding particles and a non-ideal part arising from the direct transfer by interaction forces. The second part strongly dominates when interactions are present in the fluid. As for the non-ideal pressure, it is also crucial to take into account interactions in the stress tensor as soon as the Jeans length is not resolved.

### 2.6. Thermodynamic limit

We can take the thermodynamic limit by imposing  $(N, V) \rightarrow \infty$  while keeping  $N/V = \rho$  constant. Defining  $\rho_m e$  the internal energy per unit volume (with  $\rho_m = \rho m$ ):

$$P = \rho k_B T - \frac{2\pi\rho^2}{3} \int_0^\infty g(r, \rho, T) \frac{d\phi(r)}{dr} r^3 dr, \quad (27)$$

$$\rho_m e = \frac{\rho k_B T}{\gamma - 1} + 2\pi\rho^2 \int_0^\infty g(r, \rho, T) \phi(r) r^2 dr, \quad (28)$$

where we have made the dependence of the radial distribution function to the external variables  $\rho$  and  $T$  explicit. Determining the EOS now reduces to the determination of  $g(r, \rho, T)$ , which can be done by three different technics in the case of liquids: calculation of the Ornstein-Zernike equation, N-body Monte-Carlo or molecular dynamic simulations, or experiments by X-ray or neutron diffraction (see Aslangul 2006). We emphasize that we implicitly assume here that an equilibrium can be reached, allowing to define a radial distribution function that does not depend on time and can be determined from external variables ( $\rho$  and  $T$ ). Strictly speaking, this might not be the case for self-gravitating systems that are collapsing, hence are not in equilibrium. This assumption then assumes that some sort of feedback stabilizes small scales allowing for the definition of an EOS for the scales that are not resolved and described by statistical mechanics. One can relax this assumption by using the dynamical equations in the BBGKY hierarchy describing the evolution of the correlations. However, as discussed in Davis & Peebles (1977), one needs to find a closure relation for the hierarchy, expressing the last N-point correlation functions as a function of the others. This closure is likely possible only at very high  $N$  in order to describe accurately the structures that are observed in the Universe (see Balian & Schaeffer 1989a,b), which would result in a complex system of dynamical equations describing the evolution of correlations. We therefore use here a pragmatic approach (similarly to the approach used for liquids in physical chemistry), assuming that an equilibrium, or more exactly a stationary state exists at small scales, and assuming that we can determine the two-point correlation function either by explicitly resolving inhomogeneities in small-scale numerical simulations (with e.g. molecular dynamics for liquids or e.g. N-body simulations for self-gravitating systems) or by using astrophysical observations.

An important point is that the thermodynamic limit in Eq. 28 is well-defined only if we get an extensive definition of the total internal energy  $E$  (or intensive for the internal energy density per unit volume  $\rho_m e$ ), i.e. the integral in the expression must converge when  $N, V \rightarrow \infty$ . Since  $\lim_{r \rightarrow \infty} g(r) = 1$ , it means that the potential from which the force derives must decrease faster than  $r^{-4}$  at infinity. This is the case for the Lennard-Jones potential, classically used to model inter-molecular forces in liquid water or molecular liquids. An interpretation of this requirement is that the interaction energy in Eq. 20 is actually not proportional to  $N^2$  but to  $N \times N_{\text{neighbors}}$ , with  $N_{\text{neighbors}}$  the number of particles involved in the short-range interactions. Therefore, the interaction energy is proportional to  $N$  and the definition of  $E$  is extensive in the thermodynamic limit. If the interactions are long-range, however, the interaction energy is really proportional to  $N^2$ . In that case, the total energy  $E$  is not extensive and we cannot use the thermodynamic limit. This problem is usually thought to prevent the use of statistical mechanics to describe systems characterized by a long-range force, like gravity. We will show in Sect. 3 how to get a correct treatment in the case of the gravitational force.

### 3. Non-ideal self-gravity

#### 3.1. Hierarchical Virial theorem

As we have seen in Sect. 2.4, characteristic length scales such as the Debye length  $\lambda_D$  or Jeans length  $\lambda_J$  can be defined to check out whether or not non-ideal (interaction) contributions should be taken into account. In the case of the electrostatic force, the Coulomb potential is split into a short-range and a long-range component,  $\phi = \exp(-r/\lambda_D)\phi + (1 - \exp(-r/\lambda_D))\phi$ . The first part corresponds to the screened Coulomb potential, due to the polarizable electron background, and the residual corresponds to the departure between the Coulomb and the screened potential (e.g. Chabrier, G. 1990). We propose to decompose the gravitational force in a similar manner.

Hydrogen atoms get gravitationally bounded e.g. in the interior of a star. Using a classical polytropic stellar model, we can define a Virial theorem that balance the internal energy in the star and the gravitational interaction energy (see e.g. Sect. 4.1). If now we consider a cluster of interacting polytropic stars, in a first approximation we can consider each star as isolated and use the previous Virial theorem to get their internal structure and then describe their collective dynamics assuming they are point mass (i.e. we neglect tidal interactions). However, one can easily see that we should not integrate the gravitational force at infinity when using the Virial theorem in a single star, otherwise we would include into the internal stellar structures some gravitational interactions that contribute to the cluster dynamics. A solution to this issue is to decompose the gravitational potential into a near-field and far-field component using a length scale  $\lambda_0$  larger than the size of a star

$$\phi = e^{-r/\lambda_0}\phi + (1 - e^{-r/\lambda_0})\phi \quad (29)$$

and we apply the Virial theorem inside a star using the near-field  $\phi_0 = \exp(-r/\lambda_0)\phi$ . We emphasize that the use of an exponential damping is arbitrary. Another possibility is to use an erf function as often done with the Coulomb interaction in physical chemistry. We can then proceed recursively on the residual part. We use now a second length scale  $\lambda_1$  in order to define a near-field  $\phi_1$  for the Virial theorem describing the dynamics inside the stellar cluster and a far-field for e.g. the dynamics of a collection of stellar clusters inside a galaxy.  $\phi_1$  is then given

by  $\exp(-r/\lambda_1)(1 - \exp(-r/\lambda_0))\phi$ . One can continue to define the gravitational energy contributing to the dynamics of the stellar clusters inside the galaxy and then the dynamics of the galaxies inside a galaxy cluster and so on. The hierarchical decomposition of the gravitational potential with a collection of length scales  $\lambda_0, \dots, \lambda_i, \dots$  is then given by

$$\begin{aligned} \phi &= \sum_{i=0}^{\infty} \phi_i \\ \phi_i &= e^{-r/\lambda_i} \prod_{j=0}^{i-1} (1 - e^{-r/\lambda_j}) \phi \end{aligned} \quad (30)$$

Note that this expansion is not without recalling the BBGKY hierarchy for the N-body problem in statistical physics, where the potential is split into a (short-range) inter-particle pair potential and a (long-range) external-field potential (see, e.g., Chavanis 2013). The series of length scales is a-priori arbitrary and for a purely self-gravitating collapsing fluid, there is no particular length scale that would physically make sense. The characteristic length scales that should be used are likely linked to feedback and support processes that define the possible Virial equilibria at different scales: AGN feedback for galaxy clusters, rotational support for galaxies, stellar feedback for molecular clouds and star clusters, and pressure support for stars. Once such a stationary state is reached, e.g. inside a star, one can account for the velocity dispersion and gravitational energy at this scale as internal degrees of freedom (similarly to an EOS) when going to a larger scale. If one neglects tidal effects, this allows to decouple the different scales based on feedback processes.

We can now use the Virial theorem defined in Sect. 2.2 to link the dynamic properties  $v_i, I_i$  of objects of mass  $m_i$  at each scale  $\lambda_i$  of the hierarchy to the corresponding gravitational interaction potential  $\phi_i$ :

$$-\langle m_i v_i^2 \rangle + \langle d^2 I_i / dt^2 \rangle / 2 = \langle \mathbf{F}_i \cdot \mathbf{r} \rangle, \quad (31)$$

in which we can replace kinetic energy by thermal energy for  $i = 0$ . As mentioned above, we emphasize that this hierarchy neglects tidal interactions. A possible extension would be to also decompose the energy going into tides, if they are not negligible at a given scale. This is likely to be the case at the scale of galaxies (see, e.g. Barnes & Hernquist 1992). For the time being, however, we will assume that these contributions represent a small correction to the total gravitational energy.

Since each term  $\langle \mathbf{F}_i \cdot \mathbf{r} \rangle$  is computed with the short-range potential  $\phi_i$ , damped by a factor  $e^{-r/\lambda_i}$ , we can now safely take the thermodynamic limit in Eq. 31, i.e.  $N, V \rightarrow \infty$ , since the integral converges. For a homogeneous and isotropic correlated fluid, this term is given by

$$\langle \mathbf{F}_i \cdot \mathbf{r} \rangle = 2\pi\rho^2 \int_0^{\infty} g(r) \frac{d\phi_i(r)}{dr} r^3 dr. \quad (32)$$

Similarly, the total mechanical energy of the system at a scale  $\lambda_i$  is given by

$$E_{m,i} = \langle m_i v_i^2 / 2 \rangle + \langle H_{\text{int},i} \rangle, \quad (33)$$

where we can take the thermodynamic limit for the interaction energy:

$$\langle H_{\text{int},i} \rangle = 2\pi\rho^2 \int_0^{\infty} g(r) \phi_i(r) r^2 dr \quad (34)$$

We will see in the next section that a similar decomposition can be used to define non-ideal self-gravitating hydrodynamics in numerical simulations.

### 3.2. Non-ideal self-gravitating hydrodynamics

A standard strategy to obtain a large-scale hydrodynamic model of complex multi-phasic systems relies on the homogenization procedure, by averaging volumes of characteristic size  $\lambda$  (Whitaker 1998). One can then decompose the interaction potential into a near-field and a far-field contribution, using this characteristic scale. However, in numerical simulations, as soon as the grid size (or the kernel extension in SPH methods) is such that  $\Delta x < \lambda$ , inhomogeneities at scales smaller than  $\lambda$  have no physical meaning in such a homogenized model that is only valid at scales larger than  $\lambda$ .

In numerical simulations, it is then natural to use the grid resolution  $\Delta x$  as the characteristic length to split the gravitational interaction

$$\phi(r) = e^{-r/\Delta x} \phi(r) + (1 - e^{-r/\Delta x}) \phi(r) \quad (35)$$

We can then define a near-field  $\phi_{\text{int}}(r) = \exp(-r/\Delta x)\phi(r)$  to handle the non-ideal effects in the EOS inside the simulation control volumes, and a far-field  $\phi_{\text{ext}}(r) = (1 - \exp(-r/\Delta x))\phi(r)$  to define the external force between the simulation control volumes. Following Irving & Kirkwood (1950), the Navier-Stokes equations for a non-ideal fluid can be derived from the Liouville equation in the BBGKY hierarchy and in the case of a self-gravitating fluid are given by

$$\begin{aligned} \frac{\partial \rho_m}{\partial t} + \nabla \cdot (\rho_m \mathbf{u}) &= 0, \\ \frac{\partial \rho_m \mathbf{u}}{\partial t} + \nabla \cdot (\rho_m \mathbf{u} \otimes \mathbf{u} + \sigma) &= \mathbf{F}_{\text{ext}}, \\ \frac{\partial \rho_m E}{\partial t} + \nabla \cdot (\rho_m \mathbf{u} E + \sigma \cdot \mathbf{u}) &= \mathbf{F}_{\text{ext}} \cdot \mathbf{u}, \end{aligned} \quad (36)$$

using the following relations for  $E$  and  $\sigma$

$$\begin{aligned} E &= e + \frac{1}{2} \mathbf{u}^2, \\ \sigma_{ij} &= - \left( P + \left( \frac{2}{3} \eta - \chi \right) \sum_k \partial_k u_k \right) \delta_{ij} + \eta (\partial_i u_j + \partial_j u_i), \end{aligned} \quad (37)$$

in which the non-ideal (internal) quantities are given by

$$\begin{aligned} P &= \rho k_B T - \frac{2\pi\rho^2}{3} \int_0^\infty g(r) \frac{d\phi_{\text{int}}(r)}{dr} r^3 dr \\ \rho_m e &= \frac{\rho k_B T}{\gamma - 1} + 2\pi\rho^2 \int_0^\infty g(r) \phi_{\text{int}}(r) r^2 dr \\ \eta &= \frac{1}{2} \rho_m D + \frac{\pi}{15D} \rho^2 \int_0^\infty \psi_2(r) g(r) \frac{d\phi_{\text{int}}(r)}{dr} r^3 dr \\ \chi &= \frac{1}{3} \rho_m D + \frac{\pi}{9D} \rho^2 \int_0^\infty \psi_0(r) g(r) \frac{d\phi_{\text{int}}(r)}{dr} r^3 dr \end{aligned}$$

$$\text{with } \phi_{\text{int}}(r) = -\frac{Gm^2}{r} e^{-r/\Delta x}, \quad (38)$$

with  $\psi_2(r)$  and  $\psi_0(r)$  given by Eq. 26. The external force is defined by an integral form on the whole simulation domain  $V_{\text{sim}}$

$$\begin{aligned} \mathbf{F}_{\text{ext}}(\mathbf{x}) &= -\rho(\mathbf{x}) \nabla_{\mathbf{x}} (\Phi_{\text{ext}}(\mathbf{x})), \\ \Phi_{\text{ext}}(\mathbf{x}) &= \int_{V_{\text{sim}}} \phi_{\text{ext}}(|\mathbf{x} - \mathbf{x}'|) \rho(\mathbf{x}') dV_{\text{sim}}, \\ \text{with } \phi_{\text{ext}}(r) &= -\frac{Gm^2}{r} (1 - e^{-r/\Delta x}) \end{aligned} \quad (39)$$

As for the Virial theorem in the previous section, all the integrals in the EOS quantities are defined with the damped potential  $\phi_{\text{int}}(r) = e^{-r/\Delta x} \phi(r)$ . Hence, all these integrals are well-defined

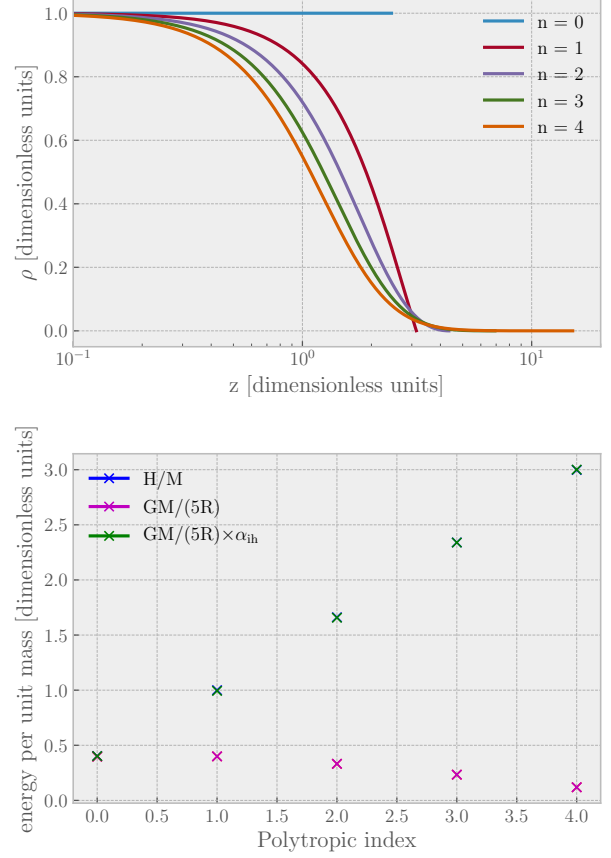


Fig. 3: Top: density profiles solutions to the Lane-Emden equation with different polytropic indexes  $n$ . Bottom: total enthalpy per unit mass compared to gravitational interaction energy per unit mass assuming either a homogeneous density profile or accounting for inhomogeneities. Blue and green crosses are indistinguishable.

and converge in the thermodynamic limit. When  $\Delta x \ll \lambda_J$  and notably in the limit  $\Delta x \rightarrow 0$ , we have  $\phi_{\text{int}}(r) \rightarrow 0$  and  $\phi_{\text{ext}}(r) \rightarrow \phi(r)$ , which means that all the gravitational force is entirely resolved externally and the non-ideal contributions to the fluid EOS given by Eqn.(38) are negligible: we recover then the classical (ideal) form of the Navier-Stokes equations for a self-gravitating fluid. As soon as  $\Delta x > \lambda_J$ , however, the non-ideal contributions to the EOS due to interactions within the control volumes must be included for a correct calculation of the gravitational energy of the whole system.

## 4. Applications

### 4.1. Impact of inhomogeneities on the Virial theorem

The Virial theorem is usually applied in astrophysics in a simplified way. We define the total mass  $M = Nm$ , and the average total energy  $\langle E/M \rangle$ , kinetic energy  $\langle E_{\text{kin}}/M \rangle$  and potential energy  $\langle E_p/M \rangle$  per unit mass. The Virial theorem, assuming that the particles are gravitationally bound in a sphere of radius  $r_{\text{bound}}$ , is usually evaluated with these quantities per unit mass

$$\begin{aligned} \langle E/M \rangle &= \langle E_{\text{kin}}/M \rangle + \langle E_p/M \rangle, \\ -2\langle E_{\text{kin}}/M \rangle &= \langle E_p/M \rangle \approx -\frac{GM}{r_{\text{bound}}}. \end{aligned} \quad (40)$$

One can see that the use of a radius  $r_{\text{bound}}$  is similar to the decomposition into near- and far-fields that we have introduced in Sect. 3.1. It defines a scale up to which the gravitational energy is considered to contribute to the Virial balance, while the rest is implicitly assumed to contribute to larger-scale dynamics. However, one also sees that this form of the Virial theorem contains no information about the sub-structures present within the bound volume: only the total mass and size of the system enters into the Virial equation. This latter thus ignores non-ideal effects due to correlations induced by these sub-structures.

In order to show the importance of inhomogeneities in the Virial theorem, we will apply it, as a simple semi-analytical example, to the case of a polytropic stellar structure. In such a case, we can explicitly compute  $P_2(\mathbf{r}, \mathbf{r}')$  by computing semi-analytically an inhomogeneous density field and compare the result with a homogeneous assumption on the Virial theorem. A polytropic stellar structure can be calculated by the Lane-Emden equation

$$\frac{1}{z^2} \frac{d}{dz} \left( z^2 \frac{dw}{dz} \right) + w^n = 0, \quad (41)$$

with  $\rho = \rho_c w^n$ ,  $P = K\rho^\gamma$ ,  $n = 1/(\gamma - 1)$  the polytropic index,  $z = Ar$ , and  $A^2 = (4\pi G/(n+1))\rho_c^{1-1/n}/K$ . We choose a dimensionless unit system in which  $\rho_c = K = G = 1$ . By solving the Lane-Emden equation for different polytropic indexes  $n < 5$ , we can compute inhomogeneous density profiles that have a finite radius  $R$  (see the top panel of Fig. 3). For a polytrope, the following Virial theorem (per unit mass) reads:

$$\begin{aligned} H/M &= 2H_{\text{int}}/M, \\ H &= \int_V \frac{\gamma}{\gamma-1} P dV, \\ M &= \int_V \rho dV, \end{aligned} \quad (42)$$

where  $H$  is the total enthalpy,  $M$  the total mass and  $H_{\text{int}}$  is given by Eq. 13 with the zero of potential energy defined at the surface of the star. For a homogeneous density profile in Eq. 13, with  $\rho = M/(4\pi R^3/3)$ , we get

$$\frac{H}{M} = \frac{GM}{5R}. \quad (43)$$

For the inhomogeneous case, as illustrated in Fig. 1, there is two possibilities for the description of the inhomogeneities. In the first case (with  $V_1$ ), these latter are resolved (for instance in high resolution simulations or observations) so that  $\rho(r)$  is not constant. In the opposite case (with  $V_2$ ),  $\rho(r)$  is constant and the (unresolved) inhomogeneities are included in the pair correlation function  $g(r)$  in our formalism. Finding out the impact of ignoring the inhomogeneities thus leads to two different possibilities. For the ‘resolved’ case, it means comparing the computation with  $\rho(r)$  not constant with the one in which  $\rho(r)$  is replaced by its mean value. For the ‘unresolved’ case, it means comparing the computation with  $g(r) \neq 1$  with the one assuming an uncorrelated fluid,  $g(r) = 1$ . The semi-analytical polytropic model allows to easily perform the first (‘resolved’) test. Indeed, since we can compute explicitly the inhomogeneous profile  $\rho(r)$  and all the necessary integral quantities, we can compare this exact solution with the one replacing  $\rho(r)$  by its mean value.

Let us now assume that an observer has only access to the total enthalpy, mass and radius of different objects and does not know whether these objects have substructures or not. The naive assumption, as explained above, is to ignore the possible inhomogeneities and assume that the density is constant,

$\rho = M/(4\pi R^3/3)$ , hence using Eq. 43 for the Virial equation. Such an assumption, however, is only correct for a polytropic index  $n = 0$ . As shown in the bottom panel of Fig. 3, for profiles  $n \neq 0$ , the error on the total energy is significant and can be up to a factor 25 for  $n = 4$ . Therefore, the assumption of a homogeneous profile within the structures will lead to a ‘missing mass problem’. For a polytropic structure, however, we can calculate semi-analytically the inhomogeneous density profile, and thus calculate exactly the contribution of inhomogeneities to the total energy. We characterize this contribution by an inhomogeneous amplification factor  $\alpha_{\text{ih}}$  which can be calculated exactly:

$$\begin{aligned} \alpha_{\text{ih}} &= \frac{N^2 \iint_{V,V'} P_2(\mathbf{r}, \mathbf{r}') \phi(|\mathbf{r} - \mathbf{r}'|) dV dV'}{N^2 \iint_{V,V'} 1/(4\pi R^3/3)^2 \phi(|\mathbf{r} - \mathbf{r}'|) dV dV'} \\ &= \frac{\iint_{V,V'} \rho(r) \rho(r') (1/|\mathbf{r} - \mathbf{r}'| - 1/|\mathbf{R} - \mathbf{r}'|) dV dV'}{\iint_{V,V'} (M/(4\pi R^3/3))^2 (1/|\mathbf{r} - \mathbf{r}'| - 1/|\mathbf{R} - \mathbf{r}'|) dV dV'}, \end{aligned} \quad (44)$$

with  $\mathbf{R}$  a vector on a sphere of radius  $R$  (the radius of the polytropic structure), used to define the zero of the gravitational potential at the stellar surface, and  $V = 4\pi R^3/3$ . In our calculation,  $N^2 P_2(\mathbf{r}, \mathbf{r}') = N^2 P_1(\mathbf{r}) P_1(\mathbf{r}') = \rho(r) \rho(r')$  for the inhomogeneous structure while the homogeneous calculation corresponds to  $N^2 P_2(\mathbf{r}, \mathbf{r}') = N^2 P_1(\mathbf{r}) P_1(\mathbf{r}') = N^2/V^2$ , with  $P_1(\mathbf{r}) = 1/V$ . We can now correct Eq. 43 to account for inhomogeneities

$$\frac{H}{M} = \frac{GM}{5R} \alpha_{\text{ih}}. \quad (45)$$

As shown in the bottom panel of Fig. 3, when taking into account this factor, we recover exactly the correct enthalpy and the correct gravitational interaction energy for the different polytropic structures (note that the green and blue crosses in the figure are indistinguishable). This simple example demonstrates that it is mandatory to account for the contribution of sub-structures to correctly evaluate interaction energies in astrophysical structures.

#### 4.2. Gravitational viscous regime and the rotation curve of galaxies

Another consequence of sub-structures and interactions is a possible transition to a viscous regime when interactions dominate at small scales. Heuristically, one can expect the rotation curve of a fluid to be strongly impacted by viscous stresses. Indeed, for a large viscosity the rotation tends to the rotation of a Taylor-Couette flow with  $u_\theta \rightarrow \Omega r$  in cylindrical coordinates.

We can explore different regimes by performing a Hilbert expansion with a small parameter  $\epsilon$  that characterizes the regime of the flow, i.e. we can take  $\epsilon$  equal to the inverse of the Reynolds number  $\text{Re}$  such that  $\epsilon \rightarrow 0$  in the inertial limit. We assume a stationary 2D stellar flow in cylindrical coordinates using either stellar hydrodynamics (see Binney & Tremaine 1987; Burkert & Hensler 1988) or gas hydrodynamics in the HI disk with the non-ideal momentum evolution equation presented in Sect. 3.2. In the case of stellar hydrodynamics, one can replace  $k_B T$  in Eq. 36 by the velocity dispersion tensor, as done in the Jeans equation, while the interaction part in the non-ideal term remains unchanged. We develop all the variables with respect to  $\epsilon$

$$\begin{aligned} \rho_m(r, \theta) &= \rho_m^0(r) + \epsilon \rho_m^1(r, \theta) + \dots \\ u_r(r, \theta) &= \epsilon u_r^1(r, \theta) + \dots \\ u_\theta(r, \theta) &= u_\theta^0(r) + \epsilon u_\theta^1(r, \theta) + \dots \end{aligned}$$



$$\begin{aligned}
 P(r, \theta) &= P^0(r) + \epsilon P^1(r, \theta) + \dots \\
 \mathbf{F}_{\text{ext}}(r, \theta) &= \mathbf{F}_{\text{ext}}^0(r) + \epsilon \mathbf{F}_{\text{ext}}^1(r, \theta) + \dots \\
 \eta &= \eta^0 + \epsilon \eta^1 + \dots
 \end{aligned}
 \quad (46)$$

where we have made the hypothesis that the zeroth order is axisymmetric with  $u_r^0 = 0$ , and verifies the condition  $\nabla(\mathbf{u}^0) = 0$ .

We can now explore the inertial regime by assuming the following dependence of the shear viscosity and pressure,  $\eta^0 \approx 0$  and  $P^0(r) \approx 0$  in the ideal regime, thus with no contribution from interactions. The zeroth order of the non-ideal Navier-Stokes equation (Eq. 36) then gives

$$\begin{aligned}
 0^{\text{th}}, r\text{-component} : \quad & \frac{-(u_\theta^0)^2}{r} = \frac{1}{\rho_m^0} F_{\text{ext},r}^0 \\
 0^{\text{th}}, \theta\text{-component} : \quad & 0 = 0,
 \end{aligned}
 \quad (47)$$

which gives the classical velocity profile  $u_\theta^0 = \sqrt{GM/r}$ , decreasing as  $r^{-1/2}$  at large distance.

In the viscous regime dominated by the non-ideal contribution, we now have  $\eta^0 \neq 0$  and  $P^0(r) \neq 0$  because of the presence of interactions and bound structures. The zeroth order of the non-ideal Navier-Stokes equation then gives

$$\begin{aligned}
 0^{\text{th}}, r\text{-component} : \quad & \frac{-(u_\theta^0)^2}{r} = -\frac{1}{\rho_m^0} \frac{\partial P^0}{\partial r} + \frac{1}{\rho_m^0} F_{\text{ext},r}^0 \\
 0^{\text{th}}, \theta\text{-component} : \quad & 0 = \eta^0 \left( \frac{1}{r} \frac{\partial}{\partial r} \left( r \frac{\partial u_\theta^0}{\partial r} \right) - \frac{u_\theta^0}{r^2} \right).
 \end{aligned}
 \quad (48)$$

We can get the velocity profile from the  $\theta$ -component of the Navier-Stokes equation. Under appropriate boundary conditions, the fluid can exhibit a Taylor-Couette flow in the viscous limit:  $u_\theta^0 = \Omega r$ . The associated centrifugal force in the  $r$ -component is then compensated by pressure gradients. We recall that the non-ideal pressure contains attractive gravitational interactions at small-scale here, hence it can compensate the centrifugal outward acceleration.

In principle, it should be possible to verify whether this interpretation is correct or not by exploring such regimes with N-body numerical simulations. The result of such a study is presented in Figure 4, from the N-body simulations of Voglis et al. (2006) who increased the total angular momentum at fixed total mass  $M$  and size  $R$ , which means that the gravitational energy  $GM/R$  is constant for all the simulations. One can see the emergence of the arm/spiral structures on a scale  $\lambda_{\text{arm}}$  smaller than  $R$ . If one cannot explore the full N-body dynamics and approximates the simulation by a fluid, the structure bounded by the spiral arms indicates that the Jeans length is smaller than the size of the system. This implies that a non-ideal description is needed when the spiral-arm structures have formed. In such a case, the gravitational interactions at small scales inside the spiral arms has to be taken into account in the viscous stress, indicating a transition to the viscous regime. Fig. 5 displays the rotation curves associated with the simulations shown in Fig. 4, assuming a half mass radius of 3 kpc and a total mass of  $10^{11} M_\odot$  for the galaxy. One can clearly identify a deviation from the inertial regime as soon as spiral-arm structures form, which corroborates the occurrence of a transition to a viscous regime.

These results also suggest that the change in the rotation curve between spiral/dwarf galaxies and some low-surface-brightness (LSB) elliptical galaxies exhibiting Keplerian profiles can be interpreted as a phase transition, from a non-viscous to a viscous regime, that depends on the presence of bound substructures in the galaxy (e.g. local clustering or spiral arms). An example of such a transition is illustrated in Fig. 6 with the observed data of Paolo et al. (2019).

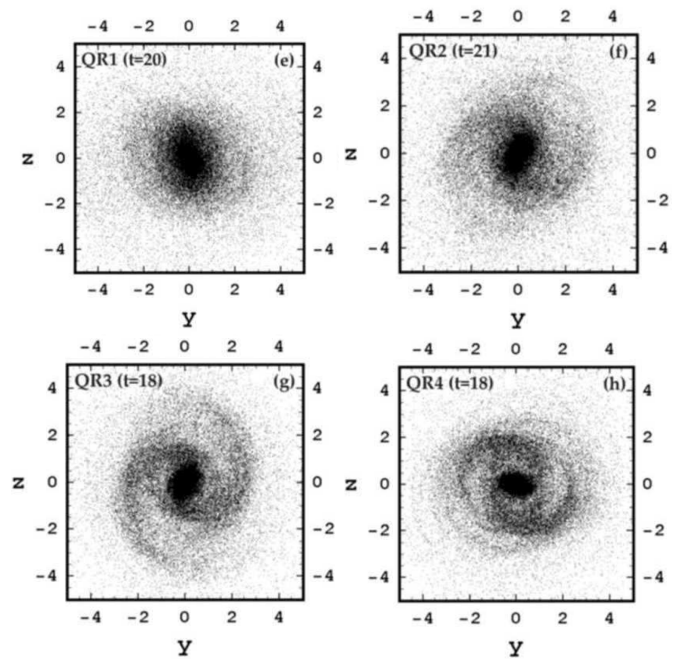


Fig. 4: Snapshots of the N-body simulations from Fig. 1 in Voglis et al. (2006). The arm/spiral structures are obtained by increasing the total angular momentum from models QR1 to QR4 for the same mass and size for all the simulations.

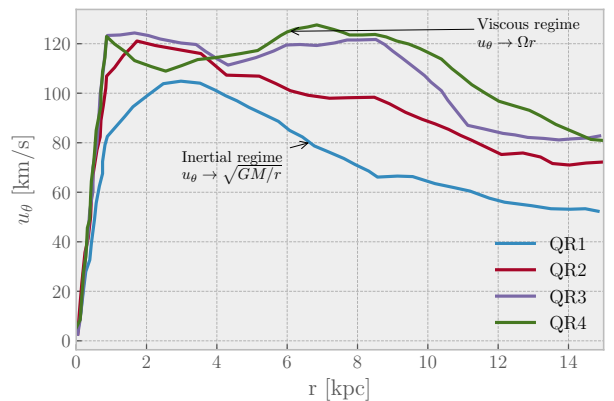


Fig. 5: Rotation curves of the different models from QR1 to QR4 from Fig. 2 in Harsoula & Kalapotharakos (2009).

#### 4.3. Non-ideal cosmology

As discussed in Sect. 2.2 and Sect. 2.3, the Poisson equation and the equivalence principle can be safely used only for uncorrelated fluids. Indeed, the Poisson and Einstein equations are not designed to account for (short-scale) correlations that can be present in a fluid. Yet, the existence of large-scale structures that have formed during the evolution of the Universe means that we are in the presence of a correlated fluid, even though at very large scales, the Universe can be considered as homogeneous and isotropic. One can even argue that, at scales characteristic of these structures, the Universe is the most correlated fluid in nature. Indeed, as shown in Fig. 7 the two-point correlation function and radial distribution function can reach values  $g(r) \approx 10^8$ , to be compared with  $g(r) = 1$  for an ideal (uncorrelated) fluid (see Fig. 7). We show below how to incorporate the effect of

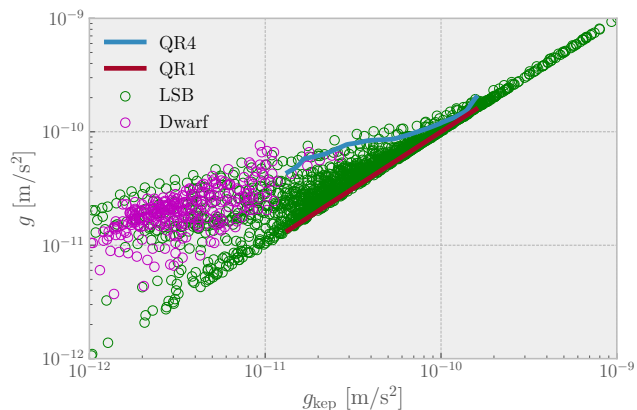


Fig. 6: Relation between total acceleration and baryonic component for LSB and dwarf galaxies (Paolo et al. 2019). Acceleration deduced from the rotation curves of the QR1 and QR4 models of Voglis et al. (2006) and Harsoula & Kalapotharakos (2009) assuming a half mass radius of 3 kpc and a total mass of  $10^{11} M_{\odot}$  for the galaxy. QR1 is taken as the reference for Keplerian rotation. The bifurcation between Keplerian rotation (QR1) and “anomalous” rotation (QR4) can be interpreted as a phase transition induced by the presence of sub-structures i.e. spiral arms that have developed in the QR4 model.

these correlations into the Friedmann equations. For simplicity, we restrict ourselves to the Newtonian limit and we do not intend to explore for now an extension of general relativity to the non-ideal regime. As such, it can be considered as a preliminary approach at this stage. As shown in many studies and textbooks (see, e.g. Peacock 1999), however, Newtonian cosmology has proved to be a very useful framework to explore various physical effects in cosmology, while keeping the calculations relatively simple.

Assuming a homogeneous and isotropic universe, we can obtain the well-known Friedmann equations from Einstein’s equation

$$\begin{aligned} H^2 + \frac{K}{a^2} &= \frac{8\pi G}{3c^2} \rho_e, \\ \dot{H} + \frac{3}{2}H^2 + \frac{K}{2a^2} &= -\frac{4\pi G}{c^2} P, \end{aligned} \quad (49)$$

with  $\rho_e$  and  $P$  the energy density and pressure,  $H = \dot{a}(t)/a(t)$  the Hubble parameter,  $K$  the Gaussian curvature and  $a(t)$  the scale factor defining the geometry of the Universe, with  $ds^2 = a(t)^2 d\Sigma^2 - c^2 dt^2$  and  $d\Sigma^2 = dr^2/(1 - Kr^2) + r^2 d\Omega^2$ . We shall consider flat geometries, with  $K = 0$ , and we define the deceleration parameter  $q = -1 - \dot{H}/H^2$ . The Friedmann equations are then given by

$$\begin{aligned} H^2 &= \frac{8\pi G}{3c^2} \rho_b, \\ q &= -1 - \frac{\dot{H}}{H^2} \approx \frac{1}{2}, \end{aligned} \quad (50)$$

with  $\rho_b$  the energy density of baryons present in the matter era. Based on the observed density of baryons, the expansion from the Hubble parameter should be of the order of 15 km/s/Mpc and the deceleration parameter close to 1/2. As a consequence, this model cannot account for the observed expansion of the Universe close to 67 km/s/Mpc from the latest data of the Planck

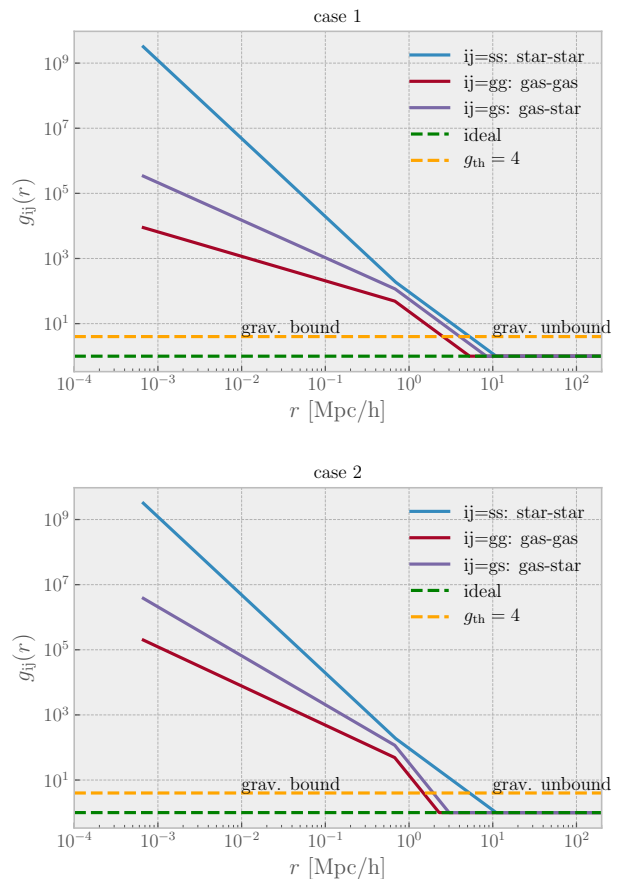


Fig. 7: Radial distribution function of stars and gas corresponding to the parameters given in Tab. 1. Case 1 corresponds to a fit of the correlation functions of the large-scale structures of the Universe at redshift 0 in the IllustrisTNG simulation from Springel et al. (2017). Case 2 uses the same stellar component but more compact sub-structures in the gas component.

mission (Planck Collaboration et al. 2018), and the acceleration of the expansion measured by Type Ia supernovae (Riess et al. 1998),  $q = -1.0 \pm 0.4$ .

To account for these discrepancies, the standard cosmological model must invoke the presence of cold dark matter (CDM) and dark energy in the form of a cosmological constant  $\Lambda$ , leading to the equations

$$\begin{aligned} H^2 &= \frac{8\pi G}{3c^2} (\rho_b + \rho_{\text{CDM}}) + \frac{\Lambda c^2}{3}, \\ q &= -1 - \frac{\dot{H}}{H^2} \approx \frac{1}{2} - \frac{\Lambda c^2}{2H}. \end{aligned} \quad (51)$$

This adjustment leads to the classical energy budget of the Universe in which baryonic matter accounts for  $\sim 5\%$ , cold dark matter for  $\sim 20\%$  and dark energy ( $\Lambda$ ) for  $\sim 75\%$ .

We will now show how to include correlations into the Friedmann equations. As mentioned above, we present for now the approach within the Newtonian limit to illustrate our point. Following Peacock (1999), we assume an ensemble of particles of mass  $m$  in a volume  $V$  of radius  $R$ , whose fluid density is assumed to be homogeneous and isotropic at very large scales, but can be correlated at smaller scales, i.e.  $P_1(\mathbf{r}) = 1/V$  but  $P_2(\mathbf{r}, \mathbf{r}') \neq P_1(\mathbf{r})P_1(\mathbf{r}')$ . The total mechanical energy of this sys-

tem, under its N-body or fluid form, is given by (see § 2.2)

$$E_m = \langle mv^2/2 \rangle + \langle H_{\text{int}} \rangle. \quad (52)$$

Similarly to  $\alpha_{\text{ih}}$  in Sect. 4.1, we define  $\alpha_{\text{ni}}$  by

$$\alpha_{\text{ni}} = \frac{\iint_{V,V'} \phi(|\mathbf{r} - \mathbf{r}'|) P_2(\mathbf{r}, \mathbf{r}') dV dV'}{\iint_{V,V'} \phi(|\mathbf{r} - \mathbf{r}'|) P_1(\mathbf{r}) P_1(\mathbf{r}') dV dV'}. \quad (53)$$

The ideal (uncorrelated) fluid hypothesis corresponds to  $\alpha_{\text{ni}} = 1$ . Eq. 52 can then be rewritten as

$$E_m = \langle mv^2/2 \rangle + \alpha_{\text{ni}} \langle H_{\text{int,ideal}} \rangle. \quad (54)$$

Following Peacock (1999), we take  $\langle mv^2/2 \rangle = M\dot{R}^2/2$  and  $\langle H_{\text{int,ideal}} \rangle = -GM^2/R$  and rewrite this equation as

$$E_m/M = \frac{\dot{R}^2}{2} - \frac{4\pi}{3} \alpha_{\text{ni}} G \rho_m R^2. \quad (55)$$

Re-arranging the different terms, we get

$$\frac{\dot{R}^2}{R^2} - \frac{2E_m/M}{R^2} = \frac{8\pi G}{3c^2} \alpha_{\text{ni}} \rho_m c^2 \quad (56)$$

In the uncorrelated case,  $\alpha_{\text{ni}} = 1$ , and with the substitutions  $R \rightarrow a$  and  $-E_m/M \rightarrow K$ , we recognize the first Friedmann equation in Eq. 50. Therefore, Eq. 56 indicates that correlations should be accounted for through a multiplicative factor  $\alpha_{\text{ni}}$  of the energy density, for a proper non-ideal generalization of the Friedmann equation (note that this could also be seen as a multiplicative factor of the gravitational constant). The last step in getting a non-ideal first Friedmann equation is to take the thermodynamic limit in  $\alpha_{\text{ni}}$ ,  $(N, V) \rightarrow \infty$  keeping  $N/V = \rho$  constant. This can be done by introducing a near-field approximation on a scale  $\lambda_H$ , i.e. replacing  $\phi$  by  $\exp(-r/\lambda_H)\phi$  in Eq. 53, or equivalently introducing a cutoff of the integrals at a radius  $r_{\text{bound}}$ , roughly of the order of  $\lambda_H$ . In the latter case, and assuming a large-scale flat, homogeneous and isotropic Universe, we get the following first non-ideal Friedmann equation

$$H_{\text{ni}}^2 = \frac{8\pi G}{3c^2} \alpha_{\text{ni}} \rho_b \quad (57)$$

with

$$\alpha_{\text{ni}} = \frac{\int_0^{r_{\text{bound}}} g(r) r dr}{\int_0^{r_{\text{bound}}} r dr}. \quad (58)$$

We can now look at the acceleration of the expansion. Since we can link the value of the Hubble parameter to the non-ideal amplification induced by bound sub-structures,  $\alpha_{\text{ni}}$ , it is natural to expect an acceleration of the expansion linked to an increase of the densities of these structures, due to the ongoing gravitational collapse. In order to derive the second non-ideal Friedmann equation, we use the first law of thermodynamics in an expanding universe

$$\frac{d(\rho_e a^3)}{dt} = -P_{\text{ni}} \frac{da^3}{dt}, \quad (59)$$

where  $P$  is a non-ideal pressure. This yields the relation  $\dot{\rho}_e + 3\dot{a}/a\rho_e = -3P\dot{a}/a$ . Using this relation and the derivation of the first non-ideal Friedmann relation, we get the non-ideal second Friedmann equation:

$$\dot{H}_{\text{ni}} + \frac{3}{2} H_{\text{ni}}^2 + \frac{K}{2a^2} = \frac{-4\pi G}{c^2} P_{\text{ni}} \alpha_{\text{ni}} + \frac{4\pi G}{3c^2 H_{\text{ni}}} \rho_e \alpha_{\text{ni}}. \quad (60)$$

Assuming a flat geometry,  $K = 0$ , we get the deceleration parameter as

$$q_{\text{ni}} = \frac{1}{2} + \frac{4\pi G}{c^2 H_{\text{ni}}} P_{\text{ni}} \alpha_{\text{ni}} - \frac{\dot{\alpha}_{\text{ni}}}{2H_{\text{ni}} \alpha_{\text{ni}}}. \quad (61)$$

The non-ideal pressure term is negligible as in the ideal case. However, we can get a negative deceleration parameter with the third term because of  $\dot{\alpha}_{\text{ni}}$ , which is positive since the densities of sub-structures are increasing with time due to the ongoing gravitational collapse. This term can then replace the contribution of the cosmological constant that needs to be introduced in the Friedmann equations to explain the acceleration of the expansion in the standard  $\Lambda$ CDM approach.

To summarize, the two non-ideal Friedmann equations (for  $K = 0$ ) in our formalism are given by:

$$\begin{aligned} H_{\text{ni}}^2 &= \frac{8\pi G}{3c^2} \alpha_{\text{ni}} \rho_b, \\ q_{\text{ni}} &= -1 - \frac{\dot{H}_{\text{ni}}}{H_{\text{ni}}^2} \approx \frac{1}{2} - \frac{\dot{\alpha}_{\text{ni}}}{2H_{\text{ni}} \alpha_{\text{ni}}}, \end{aligned} \quad (62)$$

with

$$\alpha_{\text{ni}} = \frac{\int_0^{r_{\text{bound}}} g(r) r dr}{\int_0^{r_{\text{bound}}} r dr}. \quad (63)$$

We can now estimate  $g(r)$  from available numerical simulations. We first decompose  $\alpha_{\text{ni}}$  into the dominant components of visible matter, namely gas and stars:

$$\alpha_{\text{ni}} = X_{\text{star}}^2 \alpha_{\text{ss}} + (1 - X_{\text{star}})^2 \alpha_{\text{gg}} + 2X_{\text{star}}(1 - X_{\text{star}}) \alpha_{\text{gs}}, \quad (64)$$

where  $ss$ ,  $gg$ ,  $sg$  denote the star-star, gas-gas and star-gas interaction contributions, respectively, and  $X_{\text{star}}$  denotes the mass fraction in stars relative to the total visible baryonic matter in gas and stars ( $X_{\text{star}} \approx 5\%$ ). We can parameterize the radial distribution functions for gas and stars from the auto- and cross-correlation functions of the large-scale structures of the Universe (Peebles 1980) by using simulations at redshift  $z = 0$  from (Springel et al. 2017)<sup>1</sup>, as illustrated in Fig. 7. It is important to stress that the decomposition  $\alpha_{\text{ni}}$  must be made with *squared* mass fractions and account for cross-correlations because the interaction energy depends formally on  $P_2(\mathbf{r}, \mathbf{r}')$ , that can be seen as the square of the density (similarly to Eq. 15 in Springel et al. 2017). We recall the link between the correlation function and the radial distribution function  $\xi(r) = g(r) - 1$ . The radial distribution functions can be parametrized with the simple forms

$$\begin{aligned} g_{ij}(r) &= \max\left(g_{1\text{Mpc}} \times \left(\frac{r}{1\text{Mpc}}\right)^{-\beta_0}, 1\right), & r < 1\text{Mpc} \\ &= \max\left(g_{1\text{Mpc}} \times \left(\frac{r}{1\text{Mpc}}\right)^{-\beta_1}, 1\right), & r \geq 1\text{Mpc} \end{aligned} \quad (65)$$

We assume for simplification that the radial distribution function is equal to 1 at large distances, while strictly speaking it should be slightly smaller than 1 and tend to 1 at infinity. The parameters  $g_{1\text{Mpc}}$ ,  $\beta_0$  and  $\beta_1$  are given in Table 1 for two cases. Case 1 corresponds to the fit of the correlation functions presented in Springel et al. (2017), assuming  $\xi(r) \approx g(r)$  for  $\xi(r) \gg 1$ . Case 2 has the same parametrization of the stellar component as case

<sup>1</sup> As the structures obtained in  $\Lambda$ CDM cosmological simulations represent well the observations, we use them as the reference in our calculations. In contrast to the conventional  $\Lambda$ CDM model, however, dark matter and dark energy in our formalism are in reality proxies for non-ideal effects induced by sub-structures.

	case 1				case 2		
	$g_{1\text{Mpc}}$	$\beta_0$	$\beta_1$		$g_{1\text{Mpc}}$	$\beta_0$	$\beta_1$
$g_{\text{gg}}$	50	0.75	1.9	$g_{\text{gg}}$	50	1.2	3.2
$g_{\text{gs}}$	120	1.15	1.9	$g_{\text{gs}}$	120	1.5	3.2
$g_{\text{ss}}$	200	2.40	1.9	$g_{\text{ss}}$	200	2.4	1.9

Table 1: Parameters used for the parametrization of the radial distribution function of gas and stars for case 1 and case 2. The corresponding radial distribution functions are plotted in Fig. 7.

	case 1			
	1		4	
$g_{\text{th}}$	1		4	
$\alpha_{\text{gg}}$	5.02		15.56	
$\alpha_{\text{gs}}$	6.28		21.0	
$\alpha_{\text{ss}}$	61.0		257	
$X_{\text{star}}$	0.05	0.1	0.05	0.1
$\alpha_{\text{ni}}$	5.28	5.80	16.7	18.9
$H_{\text{ni}}$	34.2	35.8	60.7	64.7
$\dot{\alpha}_{\text{ni}}$	0.12	0.13	0.20	0.21
$q_{\text{ni}}$	-1.20	-1.21	-1.12	-1.09
	case 2			
	1		4	
$g_{\text{th}}$	1		4	
$\alpha_{\text{gg}}$	16.4		36.2	
$\alpha_{\text{gs}}$	31.7		72.7	
$\alpha_{\text{ss}}$	61.0		257	
$X_{\text{star}}$	0.05	0.1	0.05	0.1
$\alpha_{\text{ni}}$	17.9	19.6	40.2	45.0
$H_{\text{ni}}$	62.9	65.8	94.3	94.3
$\dot{\alpha}_{\text{ni}}$	0.21	0.21	0.26	0.27
$q_{\text{ni}}$	-1.09	-1.09	-0.87	-0.83

Table 2: Non-ideal amplification of the different component (gas-gas, star-star, and gas-star) for two different values of the threshold  $g_{\text{th}}$  used to define the bound radius. Total non-ideal amplification  $\alpha_{\text{ni}}$  and the corresponding non-ideal Hubble parameter ( $H_{\text{ni}}$  in units of km/s/Mpc) for two different values of the star mass fraction relative to the total baryon mass in the Universe (we assume a present-day baryon density of  $0.25 \text{ particle/m}^3$ ). Estimation of  $\dot{\alpha}_{\text{ni}}$  assuming a 14-Gyr-old Universe and the corresponding non-ideal deceleration parameter  $q_{\text{ni}}$ .

1, is well constrained by observations (e.g. Li & White 2009), but has more compact sub-structures in the gas component. This modification is ad-hoc for the moment and further investigations are needed to check if its amplitude would be compatible with the observational constrains that are available for the gas component. The main point of case 2, however, is to explore the sensitivity of the non-ideal amplification to the *gas* sub-structures. We then define the bound radius  $r_{\text{bound}}$  as the minimal radius such that  $g_{ij}(r) < g_{\text{th}}$  for  $r > r_{\text{bound}}$  and we explore two values for the threshold value:  $g_{\text{th}} = 1$  and  $g_{\text{th}} = 4$ .

Table 2 gives the obtained non-ideal amplification factors for the different components for the two threshold values, as well as the total non-ideal value  $\alpha_{\text{ni}}$ . We also give the corresponding non-ideal Hubble parameter for star mass fractions  $X_{\text{star}} = 5\%$  and  $X_{\text{star}} = 10\%$ , respectively. In the most conservative case (case 1 with  $g_{\text{th}} = 1$ ), we get an overall amplification factor between 5 and 6. With a modification of the gas sub-structures (case 2 with  $g_{\text{th}} = 1$ ) or a different threshold (case 1 with  $g_{\text{th}} = 4$ ), we get a total amplification of about 20, which yields the observed value of the Hubble parameter (about 67 km/s/Mpc, Planck Collaboration et al. 2018). The last case is extreme (case

2 with  $g_{\text{th}} = 4$ ) and shows that the non-ideal model can give a very rapid expansion, depending on the contribution of substructures to the gravitational energy.

It is also interesting to look at the non-ideal amplification per component: since the stars are a lot more substructured (correlated) than the gas, the non-ideal amplification for stars is between 5 and 20 times larger than the one for the gas. This effect could thus explain observations like the bullet cluster (Markevitch et al. 2004): when stars and gas are spatially separated, the non-ideal amplification in the stellar component is significantly larger than the one in the gas. If the difference is around 20 or more, the non-ideal amplification can compensate the difference in mass fractions, potentially explaining the observed high gravitational weak-lensing related to the stellar component.

We also give in Table 2 estimations for  $\dot{\alpha}_{\text{ni}}$  and the corresponding deceleration parameter  $q_{\text{ni}}$ , assuming  $\dot{\alpha}_{\text{ni}}/\alpha_{\text{ni}} \approx \ln(\alpha_{\text{ni}})/t_u$ , with  $t_u \approx 14$  Gyr the age of the Universe. We see that the deceleration parameter is always close to the observed value  $q = -1.0 \pm 0.4$  (Riess et al. 1998). An interesting feature of this non-ideal model is that, contrary to a  $\Lambda$ CDM approach that needs to introduce two parameters  $\rho_{\text{CDM}}$  and  $\Lambda$  to explain the expansion and its acceleration, we only introduce one parameter  $\alpha_{\text{ni}}$ . We can therefore link the expansion to its acceleration and provide an analytical expression for  $q_{\text{ni}}$ , using the critical density  $\rho_c = 3H^2/8\pi G$ . Assuming the non-ideal amplification factor  $\alpha_{\text{ni}}$  explains entirely the observed present-day expansion, i.e. has varied from  $\alpha_{\text{ni}} = 1$  to  $\alpha_{\text{ni}} = \rho_c/\rho_b \approx 20$  over the age of the universe,  $t_u \sim 14$  Gyr, we can get an order-of-magnitude analytical expression:

$$q_{\text{ni}} \approx \frac{1}{2} - \frac{\ln(\rho_c/\rho_b)}{2t_u H}, \quad (66)$$

which gives a deceleration parameter  $q_{\text{ni}} = -1.06$ , compatible with the value based on type Ia supernovae ( $q = -1.0 \pm 0.4$ , Riess et al. 1998).

This value is in tension with current estimates using all cosmological constrains ( $q = -0.52 \pm 0.07$ , Planck Collaboration et al. 2018). It must be stressed, however, that the aforementioned estimates of the deceleration parameter based on the Planck results rely on the  $\Lambda$ CDM model. Using the present non-ideal cosmological formalism might relax this tension: e.g. an older universe with an age of about 20 Gyr would give a non-ideal deceleration parameter around -0.5. Another possibility is that the formation of structures has slowed down in the recent universe, because e.g. of feedback processes. Indeed, observations show that the cosmic star formation rate has decreased by almost a factor 10 since redshift  $z \sim 1-2$ , i.e. within the past  $\sim 8-10$  Gyr (Madau & Dickinson 2014). An increase of the non-ideal amplification factor of about 2 within the last 7 Gyr would put it in agreement with current estimates of  $q$ . Such a possibility could be explored in detail with numerical simulations. Nonetheless, given the fact that the physics responsible for the acceleration of the Universe remains so far mysterious, it is quite remarkable that we can get a good order of magnitude estimate of the acceleration of the expansion based on a physically intuitive and appealing argument, namely the increasing density induced by the gravitational collapse of the large-scale structures.

## 5. Discussion and conclusion

### 5.1. A non-ideal Einstein equation?

As discussed in Sect. 2.2 and Sect. 2.3, we may have to step away from the traditional forms of the Poisson and Einstein equations

to get the non-ideal Friedmann equations. For a non-relativistic fluid, the mass energy density,  $E_m = \rho c^2$ , is dominant in the zeroth component of the stress energy tensor,  $T_{00} \approx \rho c^2$ , and it would also dominate all other forms of energy, kinetic and potential:  $E_m \gg E_{\text{kin}}, E_p$ , etc... At first sight, it seems impossible for an interaction potential energy  $E_p$  to dominate over the mass energy, implying that correlations in the interaction energy should not modify the Einstein equations. It must be stressed, however, that in the non-relativistic limit of the Einstein equations, the gravitational interaction energy has a special status and should not be identified with  $E_p$ , but rather directly with the integral of  $T_{00}$ . This can be seen by deriving the Poisson equation from the Einstein equations:  $\Delta\phi \approx -4\pi G T_{00}/c^2$ . The gravitational interaction energy in the non-relativistic limit is thus given by

$$\begin{aligned} H_{\text{int}} &= \frac{1}{2} \int_V \rho(\mathbf{r}) \phi(\mathbf{r}) dV \\ &\approx -\frac{1}{2} \iint_{V,V'} G \frac{\rho(\mathbf{r}) T_{00}(\mathbf{r}')/c^2}{\|\mathbf{r} - \mathbf{r}'\|} dV dV', \end{aligned} \quad (67)$$

which corresponds to the uncorrelated (ideal) version of the interaction energy. Indeed, it ignores the distance between pairs of particles in the fluid since it does not depend on the correlation function. Heuristically, this explains why the contribution to the gravitational interaction energy arising from correlations should be introduced as a multiplicative factor of the mass energy (or of the gravitational constant) and not as an additional term.

Another way to see the limits of using the Einstein equation for self-gravitating correlated fluids is to look at the relativistic version of the non-ideal Navier-Stokes equations introduced in Sect. 3.2:  $\nabla_\mu T^{\mu\nu} = 0$ . As explained in Sect. 3.2, as soon as the Jeans length is not resolved (hence when the cosmological principle is applied at large scale), part of the gravitational interactions should be taken into account in the EOS of the fluid, hence in the definition of  $T^{\mu\nu}$ . The rest can be accounted for as external interactions with a mean field that can be included in the covariant derivative  $\nabla_\mu$  in the context of General Relativity. The gravitational interactions that contribute to the EOS cannot in general be included in the covariant derivative, which is another way to see that the equivalence principle for all the gravitational interactions is broken by the presence of correlations in a self-gravitating non-ideal fluid.

We stress that the concept of non-ideal self-gravity developed in the present paper does not modify the fundamental law of gravity between two point particles, which relies only on Newton's law. Furthermore, it does not contradict Poisson and Einstein theories: they always remain valid if one can have access to or compute exactly the full inhomogeneous density distributions down to the scale below which we can assume the gas to be uncorrelated (see the example of polytropic stars in §4.1). However, for a large ensemble of particles with unresolved small-scale inhomogeneities, a non-ideal modification of the Poisson and Einstein equations is required to account for the correlations between these sub-structures. It is worth pointing out that a modification of the Poisson equation because of correlations is a procedure already used in the case of the electrostatic force in the context of physical chemistry (see, e.g. Storey & Bazant 2012). In this field, Poisson and Einstein theories would be qualified as mean field theories, i.e. only valid in the uncorrelated case. A more complete theoretical approach to develop a non-ideal formalism for the Einstein equations could come from two routes. Either from a homogenization procedure of the inhomogeneous Einstein equations, a path already currently explored

(see, e.g. Buchert 2000, 2008), or from an extension of the concepts used in statistical mechanics, as developed in this paper, within a general relativistic framework.

## 5.2. Conclusion

Starting from the well-established BBGKY formalism, we have shown that correlations induced by bound sub-structures should be accounted for when describing the energy-mass density of the Universe. This should be done via the use of a non-ideal Virial theorem formalism and non-ideal Navier-Stokes equations. Taking into account these non-ideal effects yields an "amplification" of the gravitational interaction energy which could account, at least partly, for the missing mass problem in galaxies, clusters of galaxies, and large-scale structures in general. The strength of this model is that the radial distribution function (or the two-point correlation function) can be well determined in galaxies and the large-scale structures either by observations or by simulations.

By looking at the viscous limit of the non-ideal Navier-Stokes equations induced by the presence of small-scale interactions, we show that the presence of sub-structures (e.g. spiral arms and local clustering) can produce non-Keplerian rotation profiles that could explain the observed flat rotation curves. A consequence of this approach is to show that the observed bifurcation between spiral/dwarf galaxies and some LSB galaxies with Keplerian rotation profiles, could be explained by the presence or absence of sub-structures within these galaxies. In the context of statistical mechanics this bifurcation could be interpreted as a phase transition between two different equilibrium (viscous and non-viscous) states.

Using this non-ideal Virial theorem, we have derived non-ideal Friedmann equations, within the Newtonian limit. Using the radial distribution function of visible gas and stars obtained in large-scale simulations, we can compute the non-ideal amplification factor of gravitational mass energy and show that this factor can easily be of the order of 5 to 20 and thus could explain the observed value of the Hubble parameter. Furthermore, we show that the amplification is much stronger for the stellar component than for the gas component, which could also explain the bullet cluster observation with a high gravitational weak lensing in the stellar component compared to the gas component.

Furthermore, since most of the contribution to the value of the Hubble parameter stems from the non-ideal amplification caused by the interactions between sub-structures, this naturally explains the acceleration of the expansion of the universe, as a consequence of the ongoing collapse, thus the increasing densities of these sub-structures. An amplification factor  $\alpha_{\text{ni}} \approx 20$  during most of the lifetime of the Universe yields a deceleration parameter  $q_{\text{ni}} \approx -1$  (see Eq. 66), close to the estimates based on type Ia supernovae. To the best of our knowledge, this model is the first one able to predict a coherent value for the acceleration of the expansion of the universe with first-principle physical arguments.

Observations of the *Euclid* satellite will be crucial to probe and further constrain the radial distribution function and the non-ideal effects of self-gravitating matter at large scale. A precise characterization of these effects will be essential to build a full non-ideal cosmological model addressing all cosmological constraints (e.g. CMB data) and to reveal eventually what is really dark in our Universe.

*Acknowledgements.* We thank the anonymous referee for his/her constructive comments. We thank S. Kokh and E. Audit for co-supervising the PhD of T. Padioulet. This PhD subject is at the frontier between astrophysics and two-

phase flow simulations for the cooling system of nuclear power plants and the link between liquid statistical mechanics and gravity at large scale has emerged from this trans-disciplinary approach. They also thank CEA in general (DRF and DES in particular) for the funding of the PhD and for providing a favorable environment for trans-disciplinarity at Maison de la Simulation. PT also thanks the Astrosim 2019 school and in particular J. Rosdhal and O. Hahn for their lectures: part of the ideas presented in this paper has emerged after the school. The authors also thank F. Sainsbury-Martinez, J. Faure, T. Buchert, G. Laibe, Q. Vigneron, P. Hennebelle, F. Bournaud, D. Elbaz, D. Borgis, R. Balian, and L. Saint-Raymond for interesting discussions and useful comments on this paper. PT acknowledges supports by the European Research Council under Grant Agreement ATMO 757858.

## References

- Aslangul, C. 2006, lecture
- Balian, R. & Schaeffer, R. 1989a, A&A, 220, 1
- Balian, R. & Schaeffer, R. 1989b, A&A, 226, 373
- Barnes, J. E. & Hernquist, L. 1992, ARA&A, 30, 705
- Binney, J. & Tremaine, S. 1987, Galactic dynamics
- Bogoliubov, N. N. 1946, Journal of Physics-USSR, 10, 265
- Born, M. & Green, H. S. 1946, Proceedings of the Royal Society of London. Series A. Mathematical and Physical Sciences, 188, 10
- Buchert, T. 2000, in Proceedings of 9th Workshop on General Relativity and Gravitation conference, 306–321
- Buchert, T. 2008, General Relativity and Gravitation, 40, 467
- Burkert, A. & Hensler, G. 1988, A&A, 199, 131
- Chabrier, G. 1990, J. Phys. France, 51, 1607
- Chavanis, P. H. 2013, A&A, 556, A93
- Davis, M. & Peebles, P. J. E. 1977, ApJS, 34, 425
- de Vega, H. & Sánchez, N. 2002, Nuclear Physics B, 625, 409
- Hansen, J.-P. & McDonald, I. R. 2006, in Theory of Simple Liquids (Third Edition), third edition edn., ed. J.-P. Hansen & I. R. McDonald (Burlington: Academic Press), 11 – 45
- Harsoula, M. & Kalapotharakos, C. 2009, Monthly Notices of the Royal Astronomical Society, 394, 1605
- Irving, J. H. & Kirkwood, J. G. 1950, J. Chem. Phys., 18, 817
- Kirkwood, J. G. 1946, The Journal of Chemical Physics, 14, 180
- Kirkwood, J. G., Buff, F. P., & Green, M. S. 1949, The Journal of Chemical Physics, 17, 988
- Li, C. & White, S. D. M. 2009, MNRAS, 398, 2177
- Madau, P. & Dickinson, M. 2014, ARAA, 52, 415
- Markevitch, M., Gonzalez, A. H., Clowe, D., et al. 2004, The Astrophysical Journal, 606, 819
- Paolo, C. D., Salucci, P., & Fontaine, J. P. 2019, The Astrophysical Journal, 873, 106
- Peacock, J. 1999, Cosmological Physics, Cambridge Astrophysics (Cambridge University Press)
- Peebles, P. J. E. 1980, The large-scale structure of the universe
- Pfenniger, D. 2006, Comptes Rendus Physique, 7, 360
- Planck Collaboration, Aghanim, N., Akrami, Y., et al. 2018, arXiv e-prints, arXiv:1807.06209
- Riess, A. G., Filippenko, A. V., Challis, P., et al. 1998, AJ, 116, 1009
- Springel, V., Pakmor, R., Pillepich, A., et al. 2017, Monthly Notices of the Royal Astronomical Society, 475, 676
- Storey, B. D. & Bazant, M. Z. 2012, Phys. Rev. E, 86, 056303
- Truelove, J. K., Klein, R. I., McKee, C. F., et al. 1997, ApJ, 489, L179
- Voglis, N., Stavropoulos, I., & Kalapotharakos, C. 2006, Monthly Notices of the Royal Astronomical Society, 372, 901
- Whitaker, S. 1998, The Method of Volume Averaging, Theory and Applications of Transport in Porous Media (Springer Netherlands)
- Yvon, J. 1935, La théorie statistique des fluides et l'équation d'état, Actualités Scientifiques et Industrielles: Théories Mécaniques (Hermann & cie)